Aluminum Nitride Nanophotonic Phased Array on an 8-inch Silicon Wafer

Nanxi Li[1], Leh Woon Lim[1], Jin Xue[1], Chong Pei Ho[1], Shiyang Zhu[1], Yuan Hsing Fu[1], and Lennon Y. T. Lee[1]

*[1]Institute of Microelectronics, A*STAR (Agency for Science, Technology and Research), 2 Fusionopolis Way, 138634, Singapore*
Email address: linx1@ime.a-star.edu.sg

Abstract: A nanophotonic phased array is demonstrated on aluminum nitride photonics platform developed on an 8-inch silicon wafer. A beam spot at 1550 nm is clearly observed. Total power loss of 11.4 dB is also reported.

1. Introduction

Aluminum nitride (AlN), known as a wide bandgap material, has been used on integrated photonics platform [1,2]. Its wide bandgap enables photonics devices working in visible and ultraviolet (UV) wavelength regime [3,4], which overcomes the limitation of silicon. Furthermore, AlN has strong second order and third order nonlinear effects, which enable nonlinear optical generation [5,6]. In addition, AlN can be processed on complementary metal-oxide-semiconductor (CMOS)-compatible fabrication platform [7], which allows high volume manufacturing of photonics devices [8]. Based on AlN integrated photonics platform, different functional devices have been demonstrated, including modulator [1], harmonic generator [3], quantum emitter [9], and optical frequency comb [6,10]. In the meanwhile, there is limited report on AlN-based optical phased array (OPA), which has potential applications in 3D sensing as well as augmented reality [11].

Here, AlN-based OPA is demonstrated, to the best of our knowledge, for the first time on an 8-inch (200-mm) silicon wafer using CMOS-compatible fabrication facilities, with preliminary characterization results presented. The main beam spot from OPA can be clearly observed. Total power loss from fiber to optical beam spot is measured to be 11.4 dB. The OPA operates at 1550 nm wavelength as a proof-of-concept demonstration. With further optimization and variation of the device design parameters, the OPA can be applied in light detection and ranging (LiDAR) systems in both visible and infrared (IR) wavelength regime.

2. AlN-based nanophotonic phased array fabricated on silicon wafer

The schematic of the OPA on silicon substrate is illustrated in Fig. 1(a). Only 4 channels of emitters are drawn here for demonstration of concept while there can be more than tens of or even hundreds of emitters in the actual device. The OPA is formed by optical components including edge coupler, 1-to-2 beam splitter, waveguide taper, and grating at the end as emitter. The OPA grating period is designed to work at 1550 nm. The AlN-based OPA is fabricated on a passive AlN photonics platform developed in Institute of Microelectronics (IME). The fabrication process is similar to our earlier report [12], with process flow shown in Fig. 1(b). The fabrication starts from 8-inch silicon wafer with silicon dioxide (SiO_2) layer on top (step I). A 500-nm thick AlN layer is deposited through sputtering process, and a SiO_2 layer is deposited on top as etching hard mask (step II). After patterning of AlN, a SiO_2 layer is deposited followed by a top-surface planarization (step III). A thermal annealing process is applied at the end to reduce waveguide loss. The process is on wafer scale, with fabricated 8-inch (200-mm) wafer shown in Fig. 1(c).

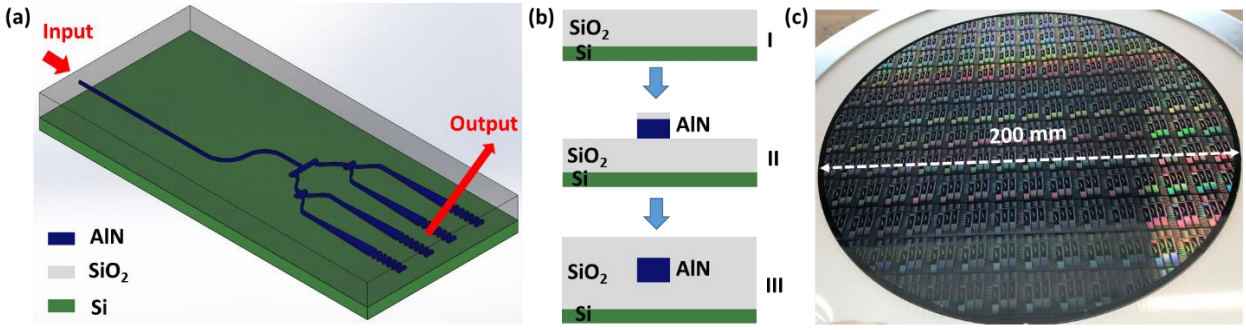

Fig. 1 (a) Schematic of AlN-based OPA on silicon substrate (drawing not to scale). Two red-color arrows indicate the direction of input and output optical beam. (b) Fabrication process flow of AlN-based OPA on a silicon substrate. Step I: Fabrication process starts from an 8-inch silicon substrate with oxide layer on top. Step II: AlN layer is deposited through sputtering process. An oxide layer is deposited on top as etching hard mask. Step III: Oxide cladding layer is deposited on top, with a planarization step to flatten the top surface. Thermal annealing is applied to reduce propagation loss of the waveguide. (c) Photograph of fabricated 8-inch (200-mm) wafer.

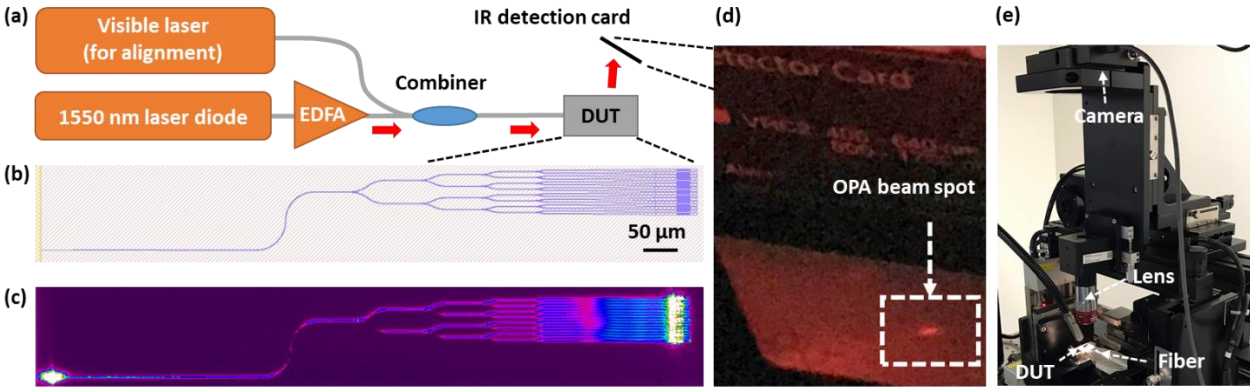

Fig. 2 (a) Schematic of OPA characterization setup. EDFA: erbium-doped fiber amplifier. DUT: device under test. (b) OPA mask layout for photolithography process. (c) Top surface image of OPA captured by camera at visible wavelength during fiber alignment using visible laser. (d) Photograph of IR card above OPA when 1550 nm laser beam is coupled into the device. OPA beam spot is highlighted in white dotted line. (e) Photograph of experiment setup used to capture the top surface image of OPA at visible wavelength as shown in (c).

3. AlN-based nanophotonic phased array characterization

The fabricated OPA device is characterized using the setup shown in Fig. 2(a). A 1550 nm laser diode cascaded with an erbium-doped fiber amplifier (EDFA) is used as light source for the device under test (DUT). A visible laser is used for alignment, to ensure optical signal is coupled into the edge coupler. A visible light camera is mounted directly above the DUT to monitor its coupling status. An IR detection card is placed above the OPA under test to visualize beam spot emitted from OPA. The OPA mask layout is illustrated in Fig. 2(b). Figure 2(c) shows an image captured by visible light camera using the setup illustrated in Fig. 2(e). From the captured image, bright scattered light at the gratings can be clearly observed when visible light is coupled into waveguide. The position of input fiber is adjusted to optimize the coupling. After alignment, the visible laser is switched off, and 1550 nm laser diode together with EDFA are switched on. A clear beam spot can be observed on IR detection card when it is placed above the OPA, as highlighted with white dotted lines in Fig. 2(d). The total power loss from fiber output to OPA beam spot is measured to be 11.4 dB (including fiber-to-chip coupling loss). Further quantitative characterization of OPA beam spot can be conducted. Also, OPA efficiency can be further improved by optimization of OPA grating design. An additional note worth mentioning is that although current OPA works in IR, working wavelength can be extended to visible, contributed by low-loss AlN waveguide demonstrated in both wavelength regimes [4,7].

4. Conclusion

To sum up, an AlN-based OPA is demonstrated on 8-inch silicon substrate for the first time. A beam spot at 1550 nm wavelength emitted by the OPA can be clearly observed using an IR detection card. Total power loss from fiber to the beam spot is measured to be 11.4 dB. Future works include quantitative characterization of OPA to obtain intensity profile of OPA beam spot. Also, based on this proof-of-concept demonstration, OPA design can be further optimized, and active tuning can be added in for high-performance AlN-based OPA working in both visible and IR wavelength regime. Potential applications include LiDAR sensing and augmented reality.

The authors acknowledge funding support from Agency for Science, Technology and Research under grant no. C220415015 and A19B3a0008. The authors also appreciate the discussions with Dr. Guanyu Chen and Dr. Yanyan Zhou.

5. References

[1] C. Xiong, *et al.* "Low-Loss, Silicon Integrated, Aluminum Nitride Photonic Circuits and Their Use for Electro-Optic Signal Processing," Nano Lett. **12**(7), 3562–3568 (2012).
[2] N. Li, *et al.* "Aluminium nitride integrated photonics: a review," Nanophotonics **10**(9), 2347–2387 (2021).
[3] X. Guo, *et al.* "Second-harmonic generation in aluminum nitride microrings with 2500%/W conversion efficiency," Optica **3**(10), 1126 (2016).
[4] X. Liu, *et al.* "Ultra-high-Q UV microring resonators based on a single-crystalline AlN platform," Optica **5**(10), 1279–1282 (2018).
[5] C. Xiong, *et al.* "Aluminum nitride as a new material for chip-scale optomechanics and nonlinear optics," New J. Phys. **14**(9), 095014 (2012).
[6] A. W. Bruch, *et al.* "Pockels soliton microcomb," Nat. Photonics **15**(1), 21–27 (2021).
[7] S. Zhu, *et al.* "Aluminum Nitride Ultralow Loss Waveguides and Push-Pull Electro-Optic Modulators for Near Infrared and Visible Integrated Photonics," in *Optical Fiber Communication Conference (OFC) 2019*, OSA Technical Digest (Optical Society of America, 2019), p. W2A.11.
[8] C. V. Poulton, *et al.* "Large-scale silicon nitride nanophotonic phased arrays at infrared and visible wavelengths," Opt. Lett. **42**(1), 21–24 (2017).
[9] T.-J. Lu, *et al.* "Bright High-Purity Quantum Emitters in Aluminum Nitride Integrated Photonics," ACS Photonics **7**(10), 2650–2657 (2020).
[10] H. Jung, *et al.* "Stokes and anti-Stokes Raman scatterings from frequency comb lines in poly-crystalline aluminum nitride microring resonators," Opt. Express **27**(16), 22246–22253 (2019).
[11] J. Notaros, *et al.* "Integrated Optical Phased Arrays: LiDAR, Augmented Reality, and Beyond," in *OSA Advanced Photonics Congress (AP) 2019 (IPR, Networks, NOMA, SPPCom, PVLED)*, OSA Technical Digest (Optical Society of America, 2019), p. IM4A.2.
[12] N. Li, *et al.* "Aluminum Nitride Photonics Platforms on Silicon Substrate," in *Conference on Lasers and Electro-Optics (2021)*, p. STh2H.3.